Inorganic Chemistry

Solvent, Anion, and Structural Effects on the Redox Potentials and UV−visible Spectral Properties of Mononuclear Manganese Corroles

Jing Shen,[†] Maya El Ojaimi,[‡] Mohammed Chkounda,[‡] Claude P. Gros,[‡] Jean-Michel Barbe,[‡] Jianguo Shao,[†] Roger Guilard,*[‡] and Karl M. Kadish*[†]

Department of Chemistry, University of Houston, Houston, Texas 77204-5003, and Université de Bourgogne, ICMUB (UMR 5260), 9 Avenue Alain Savary BP 47870, 21078 Dijon Cedex, France

A series of manganese(III) corroles were investigated as to their electrochemistry and spectroelectrochemistry in nonaqueous solvents. Up to three oxidations and one reduction were obtained for each complex depending on the solvents. The main compound discussed in this paper is the *meso*-substituted manganese corrole, (Mes$_2$PhCor)Mn, and the main points are how changes in axially coordinated anion and solvent will affect the redox potentials and UV−vis spectra of each electrogenerated species in oxidation states of Mn(III), Mn(IV), or Mn(II). The anions OAc$^-$, Cl$^-$, CN$^-$, and SCN$^-$ were found to form five-coordinate complexes with the neutral Mn(III) corrole while two OH$^-$ or F$^-$ anions were shown to bind axially in a stepwise addition to give the five- and six-coordinate complexes in nonaqueous media. In each case, complexation with one or two anionic axial ligands led to an easier oxidation and a harder reduction as compared to the uncomplexed four-coordinate species.

Introduction

A number of different metal ions have been incorporated into corroles and examined as to their electrochemical and spectroscopic properties since the mid-1990s.[1–5] The most studied of these compounds have been the transition metal derivatives of manganese,[6–13] cobalt,[14–22] and iron[23–26] due in part to the biological relevance of these metal ions and in

part to the fact that multiple metal oxidation states are possible ranging from +5 in the case of Fe and Mn to +1 in the case of iron and cobalt. Corroles with manganese, cobalt, and iron central metal ions have also been used as catalysts in a variety of reactions.[21,27–36] For example,

* To whom correspondence should be addressed. E-mail: roger.guilard@ u-bourgogne.fr (R.G.), kkadish@uh.edu (K.M.K.).
† University of Houston.
‡ Université de Bourgogne.

 (1) Erben, C.; Will, S.; Kadish, K. M. In *The Porphyrin Handbook*; Kadish, K. M., Smith, K. M., Guilard, R., Eds.; Academic Press: Burlington, MA, 2000; Vol. *2*, pp 233−300.
 (2) Paolesse, R. In *The Porphyrin Handbook*; Kadish, K. M., Smith, K. M., Guilard, R. , Eds.; Academic Press: Burlington, MA, 2000; Vol. *2*, pp 201−232..
 (3) Guilard, R.; Barbe, J.-M.; Stern, C.; Kadish, K. M. In *The Porphyrin Handbook*; Kadish, K. M., Smith, K. M., Guilard, R. , Eds.; Academic Press: Boston, MA, 2003; Vol. *18*, pp 303−349..
 (4) Gross, Z. *J. Biol. Inorg. Chem.* **2001**, *6*, 733–738.
 (5) Ghosh, A.; Steene, E. *J. Inorg. Biochem.* **2002**, *91*, 423–436.
 (6) Ou, Z.; Erben, C.; Autret, M.; Will, S.; Rosen, D.; Lex, J.; Vogel, E.; Kadish, K. M. *J. Porphyrins Phthalocyanines* **2005**, *9*, 398–412.
 (7) Steene, E.; Wondimagegn, T. W.; Ghosh, A. *J. Phys. Chem. B* **2001**, *105*, 11406–11413.
 (8) Edwards, N. Y.; Eikey, R. A.; Loring, M. I.; Abu-Omar, M. M. *Inorg. Chem.* **2005**, *44*, 3700–3708.
 (9) Bröring, M.; Hell, C.; Brandt, C. D. *Chem. Commun.* **2007**, 1861–1862.
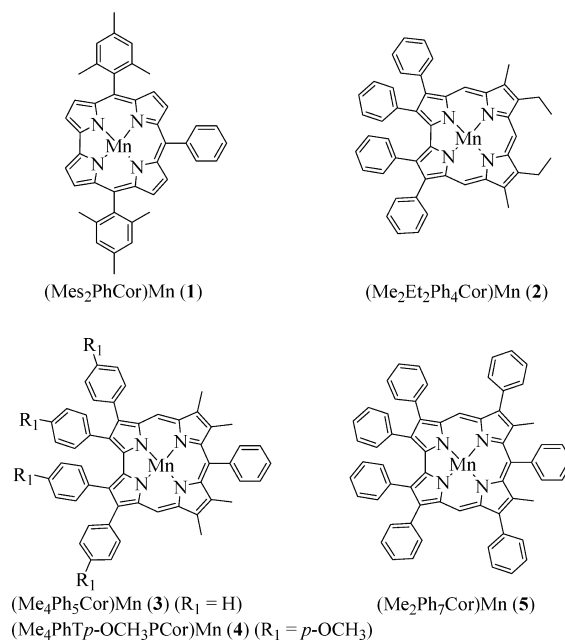 (10) Xia, M.; Liu, J.; Gao, Y.; Akermark, B.; Sun, L. *Helv. Chim. Acta* **2007**, *90*, 553–561.
 (11) Kadish, K. M.; Adamian, V. A.; Caemelbecke, E. V.; Gueletii, E.; Will, S.; Erben, C.; Vogel, E. *J. Am. Chem. Soc.* **1998**, *120*, 11986–11993.
 (12) Bröring, M.; Cordes, M.; Köhler, S. *Z. Anorg. Allg. Chem.* **2008**, *634*, 125–130.
 (13) Gross, Z.; Gray, H. B. *Comments Inorg. Chem.* **2006**, *27*, 61–72.
 (14) Kadish, K. M.; Koh, W.; Tagliatesta, P.; Sazou, D.; Paolesse, R.; Licoccia, S.; Boschi, T. *Inorg. Chem.* **1992**, *31*, 2305–2313.
 (15) Adamian, V. A. *Electrochem. Soc. Interface* **1995**, *4*, 57–58.
 (16) Will, S.; Lex, J.; Vogel, E.; Adamian, V. A.; Van Caemelbecke, E.; Kadish, K. M. *Inorg. Chem.* **1996**, *35*, 5577–5583.
 (17) Guilard, R.; Jérôme, F.; Gros, C. P.; Barbe, J.-M.; Ou, Z.; Shao, J.; Kadish, K. M. *C. R. Acad. Sci. Paris, Chimie/Chemistry* **2001**, *4*, 245–254.
 (18) Guilard, R.; Jérôme, F.; Barbe, J.-M.; Gros, C. P.; Ou, Z.; Shao, J.; Fischer, J.; Weiss, R.; Kadish, K. M. *Inorg. Chem.* **2001**, *40*, 4856–4865.
 (19) Kadish, K. M.; Ou, Z.; Shao, J.; Gros, C. P.; Barbe, J.-M.; Jérôme, F.; Bolze, F.; Burdet, F.; Guilard, R. *Inorg. Chem.* **2002**, *41*, 3990–4005.
 (20) Kadish, K. M.; Shao, J.; Ou, Z.; Gros, C. P.; Bolze, F.; Barbe, J.-M.; Guilard, R. *Inorg. Chem.* **2003**, *42*, 4062–4070.
 (21) Kadish, K. M.; Frémond, L.; Ou, Z.; Shao, J.; Shi, C.; Anson, F. C.; Burdet, F.; Gros, C. P.; Barbe, J.-M.; Guilard, R. *J. Am. Chem. Soc.* **2005**, *127*, 5625–5631.
 (22) Kadish, K. M.; Shao, J.; Ou, Z.; Zhan, R.; Burdet, F.; Barbe, J.-M.; Gros, C. P.; Guilard, R. *Inorg. Chem.* **2005**, *44*, 9023–9038.
 (23) Aviv, I.; Gross, Z. *Chem. Commun.* **2007**, 1987–1999.

Mn(III) tris(pentafluorophenyl)corrole has been shown to be a mild epoxidation catalyst[37] and also a direct precursor for the preparation of oxomanganese(V), nitridomanganese(V), and even nitridomanganese(VI) derivatives.[37,38] Langmuir−Blodgett (LB) films of a manganese(III) corrole have also been reported[39] and, in the field of molecular materials, this might be a useful approach to develop quartz microbalances with improved and very particular sensing properties.[39]

Our own interest in manganese corroles has been in elucidating their electrochemical and spectroscopic properties,[6,11] some of which closely resemble the properties of porphyrins,[40] phthalocyanines,[41,42] and related macrocycles[43–45] which have been extremely well-characterized over the years. In each of these related manganese compounds, the central ion can exist in oxidation states of +5, +4, +3, or +2, although in the case of corroles, Mn(II) derivatives have never been formally identified, in part because the reduction of Mn(III) occurs at very negative potentials and in part because a Mn(III) π-anion radical may be the product of the first reduction.[6,11]

This is investigated in the present study where we have electrochemically reduced and oxidized the series of Mn(III) corroles shown in Chart 1 and then selected (Mes$_2$PhCor)Mn **1** as a representative compound to characterize the high and

(24) Fukuzumi, S. *Kagaku* **2006**, *61*, 31–32.
(25) Van Caemelbecke, E.; Will, S.; Autret, M.; Adamian, V. A.; Lex, J.; Gisselbrecht, J.-P.; Gross, M.; Vogel, E.; Kadish, K. M. *Inorg. Chem.* **1996**, *35*, 184–192.
(26) Autret, M.; Will, S.; Caemelbecke, E. V.; Lex, J.; Gisselbrecht, J.-P.; Gross, M.; Vogel, E.; Kadish, K. M. *J. Am. Chem. Soc.* **1994**, *116*, 9141–9149.
(27) Grodkowski, J.; Neta, P.; Fujita, E.; Mahammed, A.; Simkhovich, L.; Gross, Z. *J. Phys. Chem. B* **2002**, *106*, 4772–4778.
(28) Liu, H.-Y.; Liu, L.-Y.; Zhang, L.; Ying, X.; Wang, X.-L.; Jiang, H.-F.; Chang, C.-K. *Gaodeng Xuexiao Huaxue Xuebao* **2007**, *28*, 1628–1630.
(29) Gershman, Z.; Goldberg, I.; Gross, Z. *Angew. Chem., Int. Ed.* **2007**, *46*, 4320–4324.
(30) Gao, Y.; Liu, J.; Wang, M.; Na, Y.; Åkermark, B.; Sun, L. *Tetrahedron* **2007**, *63*, 1987–1994.
(31) Mahammed, A.; Gross, Z. *Angew. Chem., Int. Ed.* **2006**, *45*, 6544–6547.
(32) Kadish, K. M.; Frémond, L.; Burdet, F.; Barbe, J.-M.; Gros, C. P.; Guilard, R. *J. Inorg. Biochem.* **2006**, *100*, 858–868.
(33) Kadish, K. M.; Shao, J.; Ou, Z.; Frémond, L.; Zhan, R.; Burdet, F.; Barbe, J.-M.; Gros, C. P.; Guilard, R. *Inorg. Chem.* **2005**, *44*, 6744–6754.
(34) Aviv, I.; Gross, Z. *Synlett* **2006**, 951–953.
(35) Collman, J. P.; Kaplun, M.; Decreau, R. A. *Dalton Trans.* **2006**, 554–559.
(36) Simkhovich, L.; Gross, Z. *Tetrahedron Lett.* **2001**, *42*, 8089–8092.
(37) Gross, Z.; Golubkov, G.; Simkhovich, L. *Angew. Chem., Int. Ed.* **2000**, *39*, 4045–4047.
(38) Golubkov, G.; Gross, Z. *J. Am. Chem. Soc.* **2005**, *127*, 3258–3259.
(39) Paolesse, R.; Di Natale, C.; Macagnano, A.; Sagone, F.; Scarselli, M. A.; Chiaradia, P.; Troitsky, V. I.; Berzina, T. S.; D'Amico, A. *Langmuir* **1999**, *15*, 1268–1274.
(40) *The Porphyrin Handbook*; Kadish, K. M., Smith, K. M., Guilard, R., Eds.; Academic Press: Burlington, MA, 2000.
(41) *The Porphyrin Handbook*, Kadish, K. M., Smith, K. M., Guilard, R., Eds.; Academic Press: Boston, MA, 2003.
(42) *Phthalocyanines Properties and Applications*; Leznoff, C. C., Lever, A. B. P., Eds.; VCH Publishers, Inc.: New York, NY, 1993.
(43) Kerber, W. D.; Goldberg, D. P. *J. Inorg. Biochem.* **2006**, *100*, 838–857.
(44) Licoccia, S.; Morgante, E.; Paolesse, R.; Polizio, F.; Senge, M. O.; Tondello, E.; Boschi, T. *Inorg. Chem.* **1997**, *36*, 1564–1570.
(45) Lansky, D. E.; Mandimutsira, B.; Ramdhanie, B.; Clausen, M.; Penner-Hahn, J.; Zvyagin, S. A.; Telser, J.; Krzystek, J.; Zhan, R.; Ou, Z.; Kadish, K. M.; Zakharov, L.; Rheingold, A. L.; Goldberg, D. P. *Inorg. Chem.* **2005**, *44*, 4485–4498.

Chart 1

(Mes$_2$PhCor)Mn (**1**)

(Me$_2$Et$_2$Ph$_4$Cor)Mn (**2**)

(Me$_4$Ph$_5$Cor)Mn (**3**) (R$_1$ = H)
(Me$_4$PhTp-OCH$_3$PCor)Mn (**4**) (R$_1$ = p-OCH$_3$)

(Me$_2$Ph$_7$Cor)Mn (**5**)

low oxidation state products in different solvents and when coordinated with different anionic axial ligands.

The electrochemistry of manganese corroles was first described in the literature for Mn(III) and Mn(IV) derivatives of octaethylcorrole (OEC), examples being (OEC)Mn^{III},[11] (OEC)Mn^{III}(py),[6] (OEC)Mn^{IV}Cl,[6] and (OEC)Mn(C$_6$H$_5$),[6] and this was followed several years later by studies of *meso*-substituted corroles with Mn(III) and Mn(IV) central ions,[7,10,30,46,47] two examples being tris(pentafluorophenyl)-corrole and *meso*-trisphenylcorrole. The air stable Mn(III) corroles could be reversibly oxidized to their Mn(IV) form while the air stable Mn(IV) derivatives were readily reduced to a Mn(III) form of the compound. Additional oxidations to give Mn(IV) π-cation radicals and dications or reduction to give a Mn(III) π-anion radical or formal Mn(II) species have also been reported and these electrode reactions are given by eqs 1–4 where Cor represents a general corrole macrocycle and the central metal ions are shown without axial ligands.

$$(\text{Cor})\text{Mn}^{III} + e \rightleftharpoons [(\text{Cor})\text{Mn}^{II}]^- \tag{1}$$

$$(\text{Cor})\text{Mn}^{III} \rightleftharpoons [(\text{Cor})\text{Mn}^{IV}]^+ + e \tag{2}$$

$$[(\text{Cor})\text{Mn}^{IV}]^+ \rightleftharpoons [(\text{Cor}^{\cdot})\text{Mn}^{IV}]^{2+} + e \tag{3}$$

$$[(\text{Cor}^{\cdot})\text{Mn}^{IV}]^{2+} \rightleftharpoons [(\text{Cor})\text{Mn}^{IV}]^{3+} + e \tag{4}$$

The electron transfer process in eq 2 has in the past been investigated either as an oxidation[6,11,46,47] or as a reduction[7,10,12,30,46] depending in large part upon the synthetic method of generating the starting compound. In some cases a four-coordinate Mn(III) species is the product of the synthesis[6] and in others it is a five-coordinate Mn(IV)

(46) Golubkov, G.; Bendix, J.; Gray, H. B.; Mahammed, A.; Goldberg, I.; DiBilio, A. J.; Gross, Z. *Angew. Chem., Int. Ed.* **2001**, *40*, 2132–2134.
(47) Fryxelius, J.; Eilers, G.; Feyziyev, Y.; Magnuson, A.; Sun, L.; Lomoth, R. *J. Porphyrins Phthalocyanines* **2005**, *9*, 379–386.

derivative such as (OEC)MnCl.[11] The half-wave potentials for reduction of (TPFC)Mn^{IV}Cl differ by 300 mV from $E_{1/2}$ values for the oxidation of (TPFC)Mn^{III} in solutions containing 0.1 M TBAP which was one evidence for metal-centered processes at these potentials.[46] This is addressed in the present paper where we demonstrate how changes in axially coordinated anion, the solvent, and the structure of corrole will affect the redox potentials and UV−vis spectra of each electrogenerated species in reactions 1–4. Previous spectral characterization of electroreduced Mn^{III} corroles (eq 1) is limited to a single study of (OEC)Mn(py) in pyridine[11] while nothing at all is known about UV−vis spectra of the doubly oxidized Mn(III) corroles (eq 3). The results of our present study should be of importance to better understand and control the chemical reactivity of mononuclear manganese corroles as well as dyads containing mono- or bis-Mn corrole macrocycles.

Experimental Section

Instrumentation. Cyclic voltammetry was carried out with an EG&G model 173 potentiostat/galvanostat. A homemade three-electrode electrochemistry cell was used and consisted of a platinum button or glassy carbon working electrode, a platinum wire counter electrode, and a saturated calomel reference electrode (SCE). The SCE was separated from the bulk of the solution by a fritted-glass bridge of low porosity which contained the solvent/supporting electrolyte mixture. All potentials are referenced to the SCE.

UV−visible spectroelectrochemical experiments were performed with an optically transparent platinum thin-layer electrode of the type described in the literature.[48] Potentials were applied with an EG&G Model 173 potentiostat/galvanostat. Time-resolved UV−visible spectra were recorded with a Hewlett-Packard Model 8453 diode array rapid-scanning spectrophotometer.

Microanalyses were performed at the Université de Bourgogne on a Fisons EA 1108 CHNS instrument. Mass spectra were obtained either with a Kratos Concept 32 S spectrometer in FAB mode (*m*-nitrobenzyl alcohol as matrix) or on a Bruker Ultraflex II instrument in MALDI-TOF reflectron mode using dithranol (1,8-dihydroxy-9[10H]-anthracene) as a matrix, or on a Bruker MicroToFQ instrument in ESI mode.

Chemicals and Reagents. Pyridine (py, 99.8%), dimethylsulfoxyde (DMSO, ≥ 99.9%), tetra-*n*-butylammonium chloride (TBACl, ≥ 99%), tetra-*n*-butylammonium fluoride (TBAF, 1.0 M solution in THF), tetra-*n*-butylammonium cyanide (TBACN, 95%), tetra-*n*-butylammonium thiocyanate (TBASCN, 98%), tetra-*n*-butylammonium hydroxide (TBAOH, 1.0 M solution in methanol) were obtained from Sigma-Aldrich Chemical Co. and used without further purification. Benzonitrile (PhCN) was purchased from Aldrich Chemical Co. and distilled over P$_2$O$_5$ under vacuum prior to use. Absolute dichloromethane (CH$_2$Cl$_2$, 99.8%) was received from EMD Chemicals Inc. and used without further purification. Tetra-*n*-butylammonium perchlorate (TBAP, ≥ 99%) and tetrabutylammonium acetate (TBAOAc, ≥ 99%) were purchased from Fluka Chemical Co. and used as received. Neutral alumina (Merck; usually Brockmann grade III, i.e., deactivated with 6% water) were used for column chromatography. Analytical thin layer chromatography was performed using Merck 60 F254 neutral Aluminum oxide gel (precoated sheets, 0.2 mm thick) or Merck 60 F254 silica gel (precoated sheets, 0.2 mm thick). Reactions were monitored by thin layer chromatography and spectrophotometry.

Synthesis of Manganese Derivatives. The structures of the investigated manganese corroles are given in Chart 1. The spectral characterization of each compound is in agreement with the proposed structure. FAB or MALDI-TOF mass spectra of complexes **1-5** show in each case the molecular peak which is consistent with the observed stability of the manganese(III) complexes.

Two main strategies can generally be used to obtain manganese corroles;[1,2] one involves cyclization of *a,c*-biladiene in the presence of a manganese salt[49] and the other involves a direct reaction of the free-base corrole with the manganese salt.[1,2,37,50] In the present study, the manganese complexes were prepared in good yields starting from the free-base corroles and either Mn$_2$(CO)$_{10}$ in toluene or Mn(OAc)$_2$·4H$_2$O in a dichloromethane/methanol mixture, both solutions being under argon. The free-base corroles (Me$_2$Et$_2$Ph$_4$-Cor)H$_3$, (Me$_4$Ph$_5$Cor)H$_3$, (Me$_4$PhT*p*-OCH$_3$PCor)H$_3$, (Me$_2$Ph$_7$Cor)H$_3$, and (Mes$_2$PhCor)H$_3$ were synthesized as previously reported.[51,52]

(5,15-Dimesityl-10-Phenylcorrole)manganese(III) (Mes$_2$-PhCor)Mn (1). A solution of 60 mg (0.098 mmol) of (Mes$_2$PhCor)H$_3$ and 96 mg of Mn(OAc)$_2$·4H$_2$O in 30 mL of DCE/MeOH 75/25 was heated under nitrogen at 85 °C for 5 h. The solvent was removed in vacuum and the residue passed through a silica column, first using methylene chloride and then methylene chloride/methanol (90/10) as eluents. After evaporation, the compound was obtained as a blackish-brown powder in 84% yield (55 mg). UV−visible (CH$_2$Cl$_2$): λ_{max} (ε, M^{-1} cm^{-1}) = 401 (27 000), 435 (25 000), 498 (9 000), 586 (6 000), 648(7 000). MS (MALDI-TOF): m/z = 662.057 $[M]^{+\cdot}$, ESI-HRMS: m/z = 662.22576 $[M]^{+\cdot}$, 662.2242 calculated for C$_{43}$H$_{35}$N$_4$Mn.

(8,12-Diethyl-7,13-dimethyl-2,3,17,18-tetraphenylcorrole)manganese(III) (Me$_2$Et$_2$Ph$_4$Cor)Mn (2). A solution of 150 mg (0.22 mmol) of (Me$_2$Et$_2$Ph$_4$Cor)H$_3$ and 141 mg (0.33 mmol) of Mn$_2$(CO)$_{10}$ in 30 mL of toluene was heated under argon at 118 °C for 4 h. The solvent was then evaporated in vacuum. The residue was first passed through a column of alumina using methylene chloride/heptane (70/30), then neat methylene chloride, and finally methylene chloride/methanol (99.5/0.5). After crystallization from methylene chloride/methanol 1/1, the title compound **2** was obtained as a black powder in 18% yield (30 mg). UV−visible (CH$_2$Cl$_2$): λ_{max} (ε, M^{-1} cm^{-1}) = 394 (39 000), 456 (2 000), 484 (1 800), 579 (1 600), 604 (1 800). MS (FAB): m/z (%) 738 $[M]^{+\cdot}$, 738.25 calculated for C$_{49}$H$_{39}$N$_4$Mn. Elemental analysis: Calcd for C$_{49}$H$_{39}$N$_4$Mn,MeOH: C 77.91, H 5.62, N 7.27. Found: C 77.65, H 6.06, N 7.47.

(7,8,12,13-Tetramethyl-2,3,10,17,18-pentaphenylcorrole)manganese(III) (Me$_4$Ph$_5$Cor)Mn (3). This corrole was similarly prepared in 50% yield (55 mg) from 100 mg (0.11 mmol) of (Me$_4$Ph$_5$Cor)H$_3$ and 80 mg (0.20 mmol) of Mn$_2$(CO)$_{10}$. UV−visible (CH$_2$Cl$_2$): λ_{max} (ε, M^{-1} cm^{-1}) = 394 (53 000), 412 (48 000), 461 (27 000), 491 (24 000), 582 (22 000), 609 (21 000). MS (FAB): m/z (%) 786 $[M]^{+\cdot}$, 786.25 calculated for C$_{53}$H$_{39}$N$_4$Mn. Elemental analysis: Calcd for C$_{53}$H$_{39}$N$_4$Mn, MeOH: C 79.20, H 5.29, N 6.84. Found: C 79.03, H 4.98, N 6.71.

(2,3,17,18-Tetra(p-anisil)-7,8,12,13-tetramethyl-9-phenylcorrole)manganese(III) (Me$_4$PhT*p*-OCH$_3$PCor)Mn (4). This corrole was similarly prepared in 30% yield (60 mg) from 200 mg (0.24 mmol) of (Me$_4$PhT*p*-OCH$_3$PCor)H$_3$ and 160 mg (0.4 mmol) of Mn$_2$(CO)$_{10}$. UV−visible (CH$_2$Cl$_2$): λ_{max} (ε, M^{-1} cm^{-1}) = 402

(48) Lin, X. Q.; Kadish, K. M. *Anal. Chem.* **1985**, *57*, 1498–1501.

(49) Licoccia, S.; Paolesse, R. *Metal Complexes with Tetrapyrrole Ligands III*; Springer-Verlag: Berlin and Heidelberg, 1995.
(50) Bendix, J.; Gray, H. B.; Golubkov, G.; Gross, Z. *Chem. Commun.* **2000**, 1957–1958.
(51) Guilard, R.; Gros, C. P.; Bolze, F.; Jérôme, F.; Ou, Z.; Shao, J.; Fischer, J.; Weiss, R.; Kadish, K. M. *Inorg. Chem.* **2001**, *40*, 4845–4855.
(52) Gros, C. P.; Brisach, F.; Meristoudi, A.; Espinosa, E.; Guilard, R.; Harvey, P. D. *Inorg. Chem.* **2007**, *46*, 125–135.
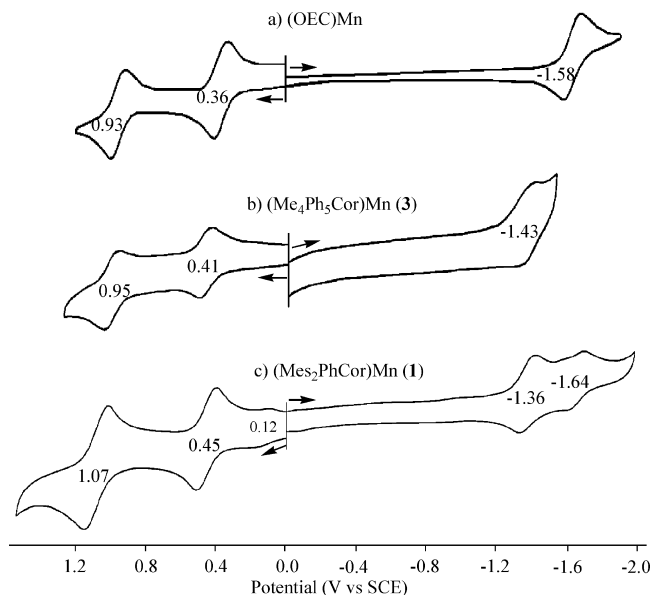
Figure 1. Cyclic voltammograms of (a) (OEC)Mn, (b) (Me$_4$Ph$_5$Cor)Mn (3), and (c) (Mes$_2$PhCor)Mn (1) in PhCN containing 0.1 M TBAP.

(45 000), 415 (14 000), 464 (25 000), 489 (20 000), 585 (17 000), 607 (17 000). MS (FAB): m/z (%) 906 $[M]^{+\bullet}$, 906.29 calculated for C$_{57}$G$_{47}$N$_4$O$_4$Mn. Elemental analysis: Calcd for C$_{57}$H$_{47}$N$_4$O$_4$Mn, MeOH: C 74.19, H 5.47, N 5.97. Found: C 74.01, H 5.17, N 5.69.

(8,12-Dimethyl-2,3,7,10,13,17,18-heptaphenylcorrole)manganese(III) (Me$_2$Ph$_7$Cor)Mn (5). This corrole was similarly prepared in 23% yield (20 mg) from 100 mg (0.11 mmol) of (Me$_2$Ph$_7$Cor)H$_3$ and 68 mg (0.16 mmol) of Mn$_2$(CO)$_{10}$. UV−visible (CH$_2$Cl$_2$): λ_{max} (ε, M^{-1} cm^{-1}) = 394 (53 000), 412 (48 000), 460 (25 000), 491 (24 000), 582 (22 000), 609 (21 000). MS (FAB): m/z (%) 910 $[M]^{+\bullet}$, 910.29 calculated for C$_{63}$H$_{43}$N$_4$Mn. Elemental analysis: Calcd for C$_{63}$H$_{43}$N$_4$Mn, MeOH: C 81.51, H 5.02, N 5.94. Found: 81.36, H 4.74, N 5.79.

Results and Discussion

Electrochemistry of 1−5 in CH$_2$Cl$_2$, PhCN and Pyridine. Cyclic voltammograms of (OEC)Mn,[6,11] (Mes$_2$PhCor)Mn 1, and (Me$_4$Ph$_5$Cor)Mn 3 in PhCN, 0.1 M TBAP are shown in Figure 1, and a summary of redox potentials is given in Table 1 for (OEC)Mn and the five corroles investigated in the current study. A third irreversible oxidation of 1−5 also occurs in PhCN and is not illustrated in the figure. This oxidation is located at peak potentials between 1.56 and 1.83 V versus SCE for a scan rate of 0.1 V/s (see exact value in Table 1).

The electrochemistry of compounds 1−5 is similar to that of (OEC)Mn[6,11] and other earlier characterized manganese corroles[7,10,30,46,47] in nonaqueous media. Each compound exhibits 1, 2, or 3 single electron abstractions in CH$_2$Cl$_2$, py, and PhCN, the exact number of which depends upon the positive potential limit of the solvent in addition to the electron-donating effect of the methyl, ethyl, or phenyl substituents. With one exception (cpd 1 in PhCN), a single one-electron reversible reduction is observed in py and PhCN, these reactions occurring over a narrow potential range of −1.34 to −1.47 V for compounds 1−5. The electroreduced forms of the Mn(III) corroles are highly

Table 1. Half-Wave Potentials (V vs SCE) of Monomeric Mn(III) Corroles in Different Nonaqueous Solvents Containing 0.1 M TBAP

		oxidation			reduction
cpd	solvent	3rd	2nd	1st	1st
(Mes$_2$PhCor)Mn (1)	CH$_2$Cl$_2$		1.00	0.32^a	
(Me$_2$Et$_2$Ph$_4$Cor)Mn (2)			0.95	0.37	
(Mes$_4$Ph$_5$Cor)Mn (3)			0.93	0.37	
(Me$_4$PhTp-OCH$_3$PCor)Mn (4)			0.90	0.32	
(Me$_2$Ph$_7$Cor)Mn (5)			0.96	0.36	
(OEC)Mn^b	PhCN	1.56^c	0.93	0.36	−1.58
(Mes$_2$PhCor)Mn (1)		1.83^c	1.07	0.45^d	−1.36, −1.64
(Me$_2$Et$_2$Ph$_4$Cor)Mn (2)		1.60^c	1.02	0.47	−1.39
(Mes$_4$Ph$_5$Cor)Mn (3)		1.62^c	0.95	0.41	−1.43
(Me$_4$PhTp-OCH$_3$PCor)Mn (4)		1.63^c	0.91	0.38	−1.42
(Me$_2$Ph$_7$Cor)Mn (5)		1.66^c	1.06	0.46	−1.34
(OEC)Mn^b	pyridine			0.32	−1.66
(Mes$_2$PhCor)Mn (1)				0.42	−1.46
(Me$_2$Et$_2$Ph$_4$Cor)Mn (2)				0.50	−1.43
(Mes$_4$Ph$_5$Cor)Mn (3)				0.47	−1.41
(Me$_4$PhTp-OCH$_3$PCor)Mn (4)				0.44	−1.47
(Me$_2$Ph$_7$Cor)Mn (5)				0.49	−1.37

^{a} Extra peak was obtained at $E_{1/2}$ = 0.03 V. ^{b} Data were taken from refs 6 and 11. ^{c} Peak potential at a scan rate of 0.1 V/s. ^{d} Extra peak was observed at $E_{1/2}$ = 0.12 V (see Figure 1c).

reactive in CH$_2$Cl$_2$, and meaningful half-wave potentials could not be obtained because of a rapid reaction of the electrogenerated anionic species with the solvent.

It is well-documented in the literature that metalloocta-ethylporphyrins are easier to oxidize and harder to reduce by 200−250 mV than the same metal complex of meso-substituted tetraphenylporphyrins.[53,54] A 200−250 mV potential difference in $E_{1/2}$ for oxidation or reduction of OECs and meso-substituted triarylcorroles with the same metal ion is often observed although this will depend upon the specific electrode reaction and specific central metal ion.[1] For example, a comparison between (OEC)Mn and (Mes$_2$PhCor)Mn 1 (Figure 1) shows that the latter compound is 90 mV harder to oxidize and 220 mV easier to reduce in PhCN than the OEC derivative with the same metal ion. The absolute potential difference in reversible half-wave potentials for oxidation and reduction of (OEC)Mn is 1.94 V in PhCN (see Table 1), a larger value than for compounds 1−5 in the same solvent where the $\Delta E_{1/2}$ values range from 1.80 to 1.86 V and show little variation with changes in the type or position of substituents on the conjugated macrocycle. This difference may suggest that at least one (and probably both) of the redox processes for cpds 1−5 are metal- rather than macrocycle-centered.

The reductions of 1−5 are easier than (OEC)Mn by 150−250 mV in PhCN or py (see Table 1) but much smaller differences in $E_{1/2}$ values are seen for the oxidation where the $\Delta E_{1/2}$ between (OEC)Mn and the newly investigated compounds are less than 100 mV and close to zero in the case of compound 4.

Because of the lack of a significant structural effect on the redox potentials of 1−5, we have selected one representative corrole to elucidate the effect of solvent and anion binding on the electrochemistry and UV−vis spectra of the

(53) Kadish, K. M.; Van Caemelbecke, E.; Royal, G. In *The Porphyrin Handbook*; Kadish, K. M., Smith, K. M., Guilard, R., Eds.; Academic Press: Burlington, MA, 2000; Vol. 8, pp 1−114.

(54) Kadish, K. M. In *Prog. Inorg. Chem.*; Lippard, S. J., Ed.; John Wiley: New York, 1986; Vol. 34, pp 435−605.
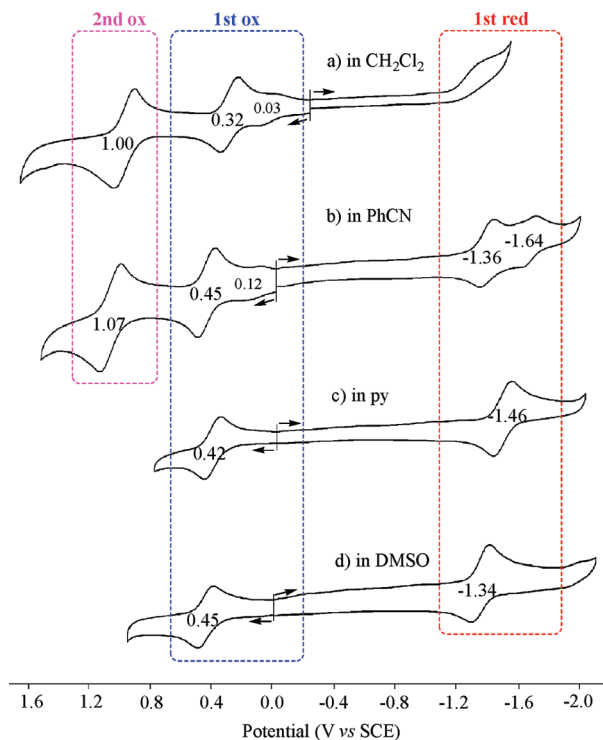
Figure 2. Cyclic voltammograms of (Mes$_2$PhCor)Mn **1** in (a) CH$_2$Cl$_2$, (b) PhCN, (c) py, and (d) DMSO containing 0.1 M TBAP.

electrogenerated products in reactions 1–4. As seen in Figure 1c, there are two "extra" redox processes obtained for cpd **1** in PhCN, one at $E_{1/2} = 0.12$ V and another at −1.64 V. These extra processes are not seen for the other corroles and cpd **1** then was therefore selected for further detailed studies on anion and solvent effect since these "extra" processes seemed to be associated with different forms of axial ligand binding under the given electrochemical conditions. This is clearly demonstrated by the cyclic voltammograms in Figure 2. As seen in the figure, compound **1** undergoes a reversible one-electron reduction in py (−1.46 V vs SCE) or DMSO (−1.34 V), an irreversible reduction in CH$_2$Cl$_2$ (because of a rapid chemical reaction with the solvent), and two reversible reductions in PhCN (−1.36 and −1.64 V) which will be shown to correspond to two different axially coordinated forms of Mn^{III}. The formal Mn^{III}/Mn^{II} and Mn^{III}/Mn^{IV} processes in each solvent are described by eqs 1 and 2 and notated as "first red" and "first ox" in the figure. The second major oxidation at 1.00 V (CH$_2$Cl$_2$) or 1.07 V (PhCN) is notated as "second ox", while the redox process with smaller currents at $E_{1/2} = 0.03$ V in CH$_2$Cl$_2$ and 0.12 V in PhCN are assigned to a rival Mn^{III}/Mn^{IV} couple (first ox) and that at −1.64 V to a different Mn^{III}/Mn^{II} couple (first red) based on experiments described in later sections of the manuscript. Each redox process of compound **1** was characterized by spectroelectrochemistry before and after electrooxidation and electroreduction as described on the following pages.

UV–vis Spectra of Neutral Compound in Different Solvents. The spectrum of **1** in neat py or neat DMSO differs from the spectrum obtained in PhCN or CH$_2$Cl$_2$ (see Figure 3 and Supporting Information, Table S1). There are two key differences. The first is that the ratio of intensities for the
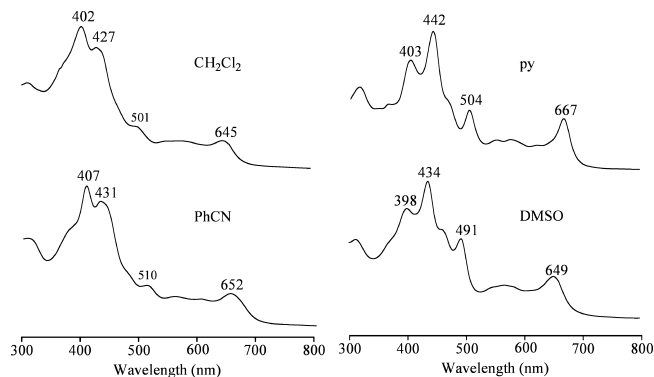

Figure 3. UV–visible spectra of (Mes$_2$PhCor)Mn **1** in different nonaqueous solvents.

split Soret band at 398 to 407 and 427 to 442 nm are reversed in py and DMSO as compared to CH$_2$Cl$_2$ and PhCN, and the second, that the intensities of the two other major bands at 491 to 510 nm and 645 to 667 nm are also larger in py and DMSO than in the other two more weakly coordinating solvents (see Figure 3 and Supporting Information, Table S1). An increased intensity visible band in the spectrum of (OMC)Mn in the presence of pyridine was earlier assigned to a formation of a five-coordinate complex in the bonding solvent,[44] and this also seems to be the case in the present study where the spectroscopically observed form of the corrole is assigned as (Mes$_2$PhCor)Mn(py) in pyridine, (Mes$_2$PhCor)Mn(DMSO) in DMSO, and (Mes$_2$PhCor)Mn in CH$_2$Cl$_2$ or PhCN. Under these conditions the first oxidation of (Mes$_2$PhCor)Mn in PhCN or CH$_2$Cl$_2$ is proposed to occur as shown in eq 2 while in py or DMSO, the prevailing electrooxidation can be described by eq 5 where S is a solvent molecule.

$$(\text{Mes}_2\text{PhCor})\text{Mn}^{III}(\text{S}) \rightleftharpoons [(\text{Mes}_2\text{PhCor})\text{Mn}^{IV}(\text{S})]^+ + e \quad (5)$$

Spectroelectrochemistry of 1. The first oxidation of manganese corroles has been described as a metal-centered reaction in the literature,[1,6,7,30,46,47] and this is what is observed for (Mes$_2$PhCor)Mn **1** after the abstraction of one electron in PhCN or DMSO (see UV–vis spectra in Figures 4a and Supporting Information, S1a). Further oxidation of the singly oxidized species leads to a decreased intensity Soret band and the appearance of a broad NIR band centered at 750−900 nm as shown in Figures 4b and Supporting Information, S1b. The latter spectra are assigned to a Mn^{IV} corrole π-cation radical[55−57] and is followed by a third irreversible reaction leading to a species assigned as a Mn^{IV} dication (spectrum not shown). These oxidations are described by eqs 2–4.

The single reduction of (OEC)Mn in pyridine was previously assigned as a macrocycle-centered reaction[6] but this seems not to be the case for (Mes$_2$PhCor)Mn in PhCN whose spectral changes during the first reduction at an applied potential of −1.50 V are shown in Figure 5a. The spectrum

(55) Fuhrhop, J. H. *Struct. Bonding (Berlin)* **1974**, *18*, 1–67.
(56) Gouterman, M. *J. Mol. Spectrosc.* **1961**, *6*, 138–163.
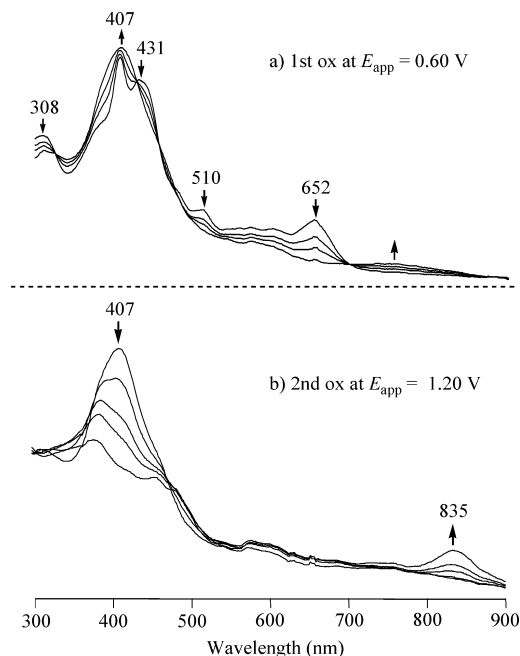(57) Perrin, M. H.; Gouterman, M.; Perrin, C. L. *J. Chem. Phys.* **1969**, *50*, 4137–4150.

Figure 4. UV−visible spectral changes of (Mes$_2$PhCor)Mn **1** during the (a) first and (b) second oxidations in PhCN containing 0.1 M TBAP.
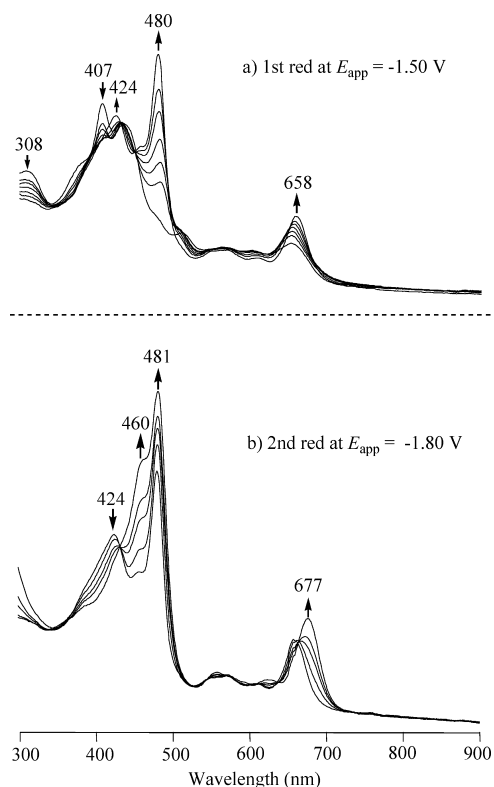

Figure 5. UV−visible spectral changes of (Mes$_2$PhCor)Mn during the (a) first and (b) second reductions in PhCN containing 0.1 M TBAP.
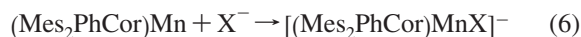
of the corrole electrogenerated at this potential has bands at 424, 480, and 658 nm, and the overall spectral changes are as would be expected for a metal-centered reaction rather than for formation of a corrole π-anion radical where significant decreases in all absorption intensities would be observed.[6] The applied potential was then shifted from −1.50 to −1.80 V, and the 481 nm band was seen to increase even more in intensity as the 424 nm band disappeared (Figure

5b). The final product at this controlled potential has bands at 460 (sh), 481 and 677 nm and also looks like a metal- rather than macrocycle-centered reduced species. Similar spectral changes are seen during controlled potential reductions in DMSO and these changes are shown in Supporting Information, Figure S2.

In the case of manganese porphyrins, the chemically or electrochemically generated Mn(II) form of the compound generally has a sharper Soret band with a larger molar absorptivity than the initial Mn(III) compound before reduction. Thus, the two electroreduction products in Figures 5a and 5b might at first be simply assigned to two different axially coordinated forms of the electrogenerated Mn(II) corrole. This is not the case, however, as will become evident after examining the UV−visible spectrum of the corrole in the presence of different axially coordinating anions. This is described on the following pages.

UV−visible Spectra of (Mes$_2$PhCor)Mn 1 in PhCN Containing Different Anions. The UV−visible spectral changes obtained upon addition of OAc$^-$ or CN$^-$ to (Mes$_2$PhCor)Mn **1** in PhCN are shown in Figure 6. Compound **1** before ligand addition has a complex spectral pattern with absorption bands at 308, 374 (sh), 407, 431, 510, 557, 601, and 652 nm but after addition of the anion in the form of TBAX the Soret band, initially at 407 nm, decreases in intensity and shifts to 388 nm (OAc$^-$) or 401 nm (CN$^-$) while the band at 431 nm changes only slightly in intensity as new bands grow in at 482 and 650 nm (OAc$^-$) or 509 and 681 nm (CN$^-$). The same spectral pattern before and after addition of CN$^-$ or OAc$^-$ is obtained in PhCN solutions containing 0.1 M TBAP, and this suggests that ClO$_4$$^-$, present as a supporting electrolyte in the electrochemical studies, does not coordinate to the Mn(III) center as is the case for the other anions.

Similar spectral changes were seen upon addition of Cl$^-$ or SCN$^-$ to (Mes$_2$PhCor)Mn **1** in PhCN, and Hill-plots were used to analyze the data as a function of added anion to calculate the number of axially coordinated ligands and anion binding constants. The diagnostic log−log plots are shown in Figure 6 and indicate that one and only one OAc$^-$ or CN$^-$ axial ligand binds to the Mn(III) center under the given solution conditions. The spectrum of the five-coordinate corrole with bound OAc$^-$ has major absorption bands at 388, 431, 482, and 650 nm (Figure 6a), and a binding constant of log$K$ = 4.5 is calculated for the reaction given in eq 6.

$$(Mes_2PhCor)Mn + X^- \rightarrow [(Mes_2PhCor)MnX]^- \quad (6)$$

The five-coordinate CN$^-$ adduct, [(Mes$_2$PhCor)Mn(CN)]$^-$, has bands at 401, 440, 509, and 681 nm (Figure 6b) and a log$K$ of 4.7 was calculated for this ligand addition reaction. Similar spectral changes are seen when SCN$^-$ or Cl$^-$ are added to **1** in PhCN (Supporting Information, Figure S3) and again the log−log plot indicates the addition of a single anion to give [(Mes$_2$PhCor)MnX]$^-$ where log$K$ = 4.8 (Cl$^-$) or 4.2 (SCN$^-$).
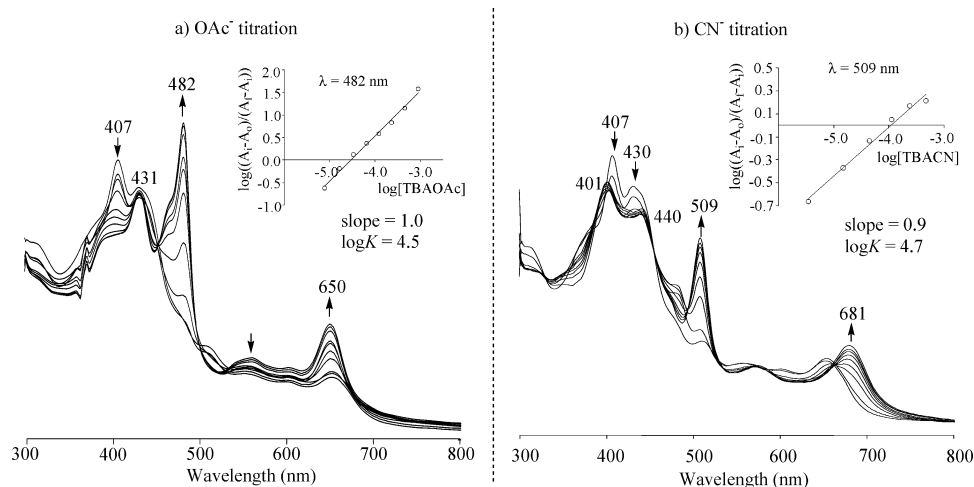
Figure 6. UV−visible spectral changes of (Mes$_2$PhCor)Mn **1** in PhCN during addition of (a) TBAOAc or (b) TBACN to solution.
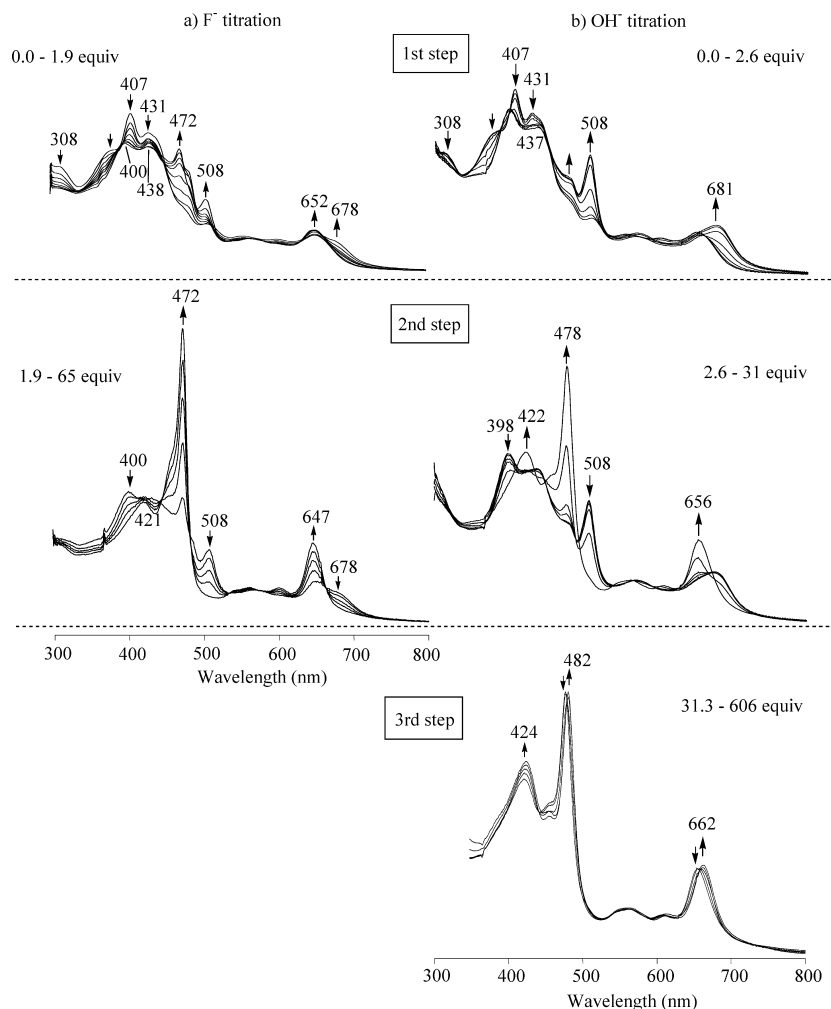

Figure 7. UV−visible spectral changes of (Mes$_2$PhCor)Mn **1** during addition of (a) TBAF or (b) TBAOH to PhCN.

Unlike OAc$^-$, Cl$^-$, CN$^-$, or SCN$^-$, the addition of F$^-$ or OH$^-$ to **1** in PhCN results in more than one set of spectral changes, each with well-defined isosbestic points as shown in Figure 7. The first change is complete after addition of 1.9 equiv F$^-$ or 2.6 equiv OH$^-$ and the second after addition of 65 equiv F$^-$ or 31 equiv OH$^-$. A third and still unexplained reaction is also obtained after further addition of OH$^-$ ion.

The first product formed after addition of OH$^-$ or F$^-$ to **1** in PhCN (Figure 7) has a UV−visible spectrum similar to that obtained upon addition of OAc$^-$, Cl$^-$, CN$^-$, or SCN$^-$ to **1** in the same solvent (see Figures 6 and Supporting Information, Figure S3). These ligand addition reactions are described by eq 6 where the corrole is represented as uncomplexed in PhCN. The second set of spectral changes

Table 2. UV-visible Spectral Data of (Mes₂PhCor)Mn Complexes **1** in PhCN Containing Different Anions

formula	X^-	λ, nm ($\varepsilon \times 10^{-4}$ M^{-1} cm^{-1})			
		I	II	III[a]	IV
(Cor)Mn^{IIIb}	none	407 (3.3)	431 (2.9)	510 (1.0)	652 (0.8)
[(Cor)Mn^{III}X]$^-$	OAc$^-$	388 (2.1)	431 (2.5)	**482** (3.3)	650 (1.0)
	Cl$^-$	393 (2.4)	435 (2.8)	**489** (3.2)	656 (1.1)
	SCN$^-$	402 (2.9)	440 (3.0)	**499** (1.9)	660 (0.9)
	CN$^-$	401 (2.9)	440 (2.7)	**509** (2.4)	681 (1.1)
	F$^-$	400^c	438^c	**508**^{c}	678^c
	OH$^-$	398 (2.9)	437 (2.7)	**508** (2.1)	681 (0.9)
[(Cor)Mn^{III}X₂]$^{2-}$	F$^-$		421 (2.5)	**472** (5.8)	647 (1.7)
	OH$^-$		422 (3.1)	**478** (4.4)	656 (1.5)

[a] Bands in bold print are designated as "marker bands" for axial coordination. *[b]* Other bands located at 308, 374sh, 557 and 601 nm (see Figure 3). *[c]* Transient species, ε cannot be determined.

in Figure 7 are described by eq 7 and occur only for X = OH$^-$ and F$^-$.

$$[(\text{Mes}_2\text{PhCor})\text{MnX}]^- + X^- \rightarrow [(\text{Mes}_2\text{PhCor})\text{MnX}_2]^{2-} \quad (7)$$

The spectra of the six-coordinate bis-hydroxide and bis-fluoride products in reaction 6 are similar in that each has an intense band at 472−478 nm and two weaker bands at 421−422 and 647−656 nm. The exact values of λ_{nm} and ε are listed in Table 2 along with spectral data for the monoadducts, [(Mes₂PhCor)MnF]$^-$ and [(Mes₂PhCor)Mn-(OH)]$^-$, both of which closely resemble the spectrum of [(Mes₂PhCor)Mn(CN)]$^-$ displayed in Figure 6b.

In summary, two types of UV−visible spectral changes are obtained upon addition of anionic axial ligands to (Mes₂PhCor)Mn **1** in PhCN. The first is for SCN$^-$, CN$^-$, Cl$^-$, and OAc$^-$ which forms only monoadducts with (Mes₂PhCor)Mn and gives the five-coordinate complex. The second is for F$^-$ and OH$^-$ where a stepwise formation of mono- and bis-adducts occurs. The five-coordinate complex has four bands at 388−407, 431−440, 482−509, and 650−681 nm while the six-coordinate species has three bands at 421−422, 472−478, and 647−656 nm which are not seen
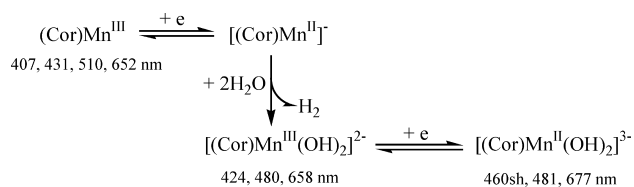
or are less intense in the spectrum of the monoadduct. The latter type of spectrum is identical to the UV−visible spectrum generated after reduction of **1** at −1.50 V in PhCN (Figure 5a), thus suggesting the two species present in solution are the same under the different experimental conditions.

As indicated above, the first electroreduction product of **1** in PhCN (see Figure 5a) has a UV−visible spectrum almost identical to that of the bis-OH$^-$ species formed in the absence of an electrochemical reaction (see Figure 7). A comparison of the two spectra is shown in Chart 2 where the only difference between the two solution conditions is the presence of the non-coordinating 0.1 M TBAP under the electrochemical conditions. The similarity between the two spectra leaves no doubt that the same form of the corrole is present under both experimental conditions. In the case of Mn(III) porphyrins, hydroxide ion is known to catalytically generate the Mn(II) form of the compound,[58,59] but this seems highly unlikely in the present case given the extremely negative potential for the first corrole reduction in PhCN, namely −1.36 V versus SCE, 1100 mV more negative than $E_{1/2}$ for reduction (TPP)Mn^{III}Cl under the same solution conditions.[60]

A more likely sequence of events involves generation of the bis-OH$^-$ Mn(III) corrole after reaction of the singly reduced corrole with trace water in PhCN. The proposed mechanism for this reaction is shown in Scheme 1 where the first electron transfer at −1.36 V is a Mn(III)/Mn(II) reaction of the uncoordinated compound in solution and the second at −1.64 V involves reduction of the homogeneously generated [(Mes₂PhCor)Mn^{III}(OH)₂]$^{2-}$ to its Mn(II) form at the electrode surface. A similar sequence of steps has previously been observed upon reduction of Si^{IV} or Ge^{IV} porphyrins in nonaqueous media[61–63] and was confirmed in the present study by monitoring the electroreduction of **1** in PhCN containing 2 equiv of TBAOH, the same conditions for generation of the spectrum in the lower part of Chart 2. In this solution, only a single reduction is observed at a potential close to that of −1.64 V. Thus, the behavior of

Chart 2

7724 Inorganic Chemistry, Vol. 47, No. 17, 2008

Scheme 1

compound **1** in PhCN is remarkable not only by the sequence of steps shown in Scheme 1 but also by the fact that this is the first direct evidence for generation of a Mn(II) corrole as opposed to a Mn(III) corrole π-anion radical.

The electrogenerated Mn(II) species is extremely reactive in its uncomplexed form, not only in PhCN but also in CH_2Cl_2 where a rapid reaction with the chlorinated solvent is shown to occur. This contrasts with the enhanced stability of the electroreduced species in pyridine where reduction is proposed to occur at the conjugated macrocycle. A well-defined cyclic voltammogram with only a single reduction process is obtained (Figure 2) and the UV–visible spectrum after reduction at −1.80 V (Figure 8) is quite different than that in PhCN (Figure 5) or DMSO (Supporting Information, Figure S2). The strong binding of pyridine to (Mes₂PhCor)-Mn leads not only to a change in the site of reduction but also prevents a chemical reaction of the electrogenerated species because of a blocking of the axial positions on the manganese center.

Anion Effect on the Electrochemistry in PhCN and Pyridine. As described earlier in the manuscript, Cl^-, OAc^-, CN^-, and SCN^- all form monoadducts with the Mn^{III} form of corrole and have binding constants between $10^{4.1}$ and $10^{4.8}$ for the reaction given in eq 6. Thus, the electroactive species, represented as $[(Mes_2PhCor)Mn^{III}X]^-$ after coordination, is negatively charged and should be harder to reduce and easier to oxidize than the corrole not having a bound anion, either (Mes₂PhCor)Mn in PhCN and CH_2Cl_2 or (Mes₂PhCor)Mn(S) in pyridine and DMSO. This is exactly what is observed as shown in Figure 9a which compares cyclic voltammograms of millimolar solutions of **1** in PhCN with and without added chloride ion in solution. The first oxidation in PhCN containing 1.0 M TBACl occurs at $E_{1/2} = 0.10$ V as compared to $E_{1/2} = 0.45$ V in PhCN, 0.1 M TBAP, a 350
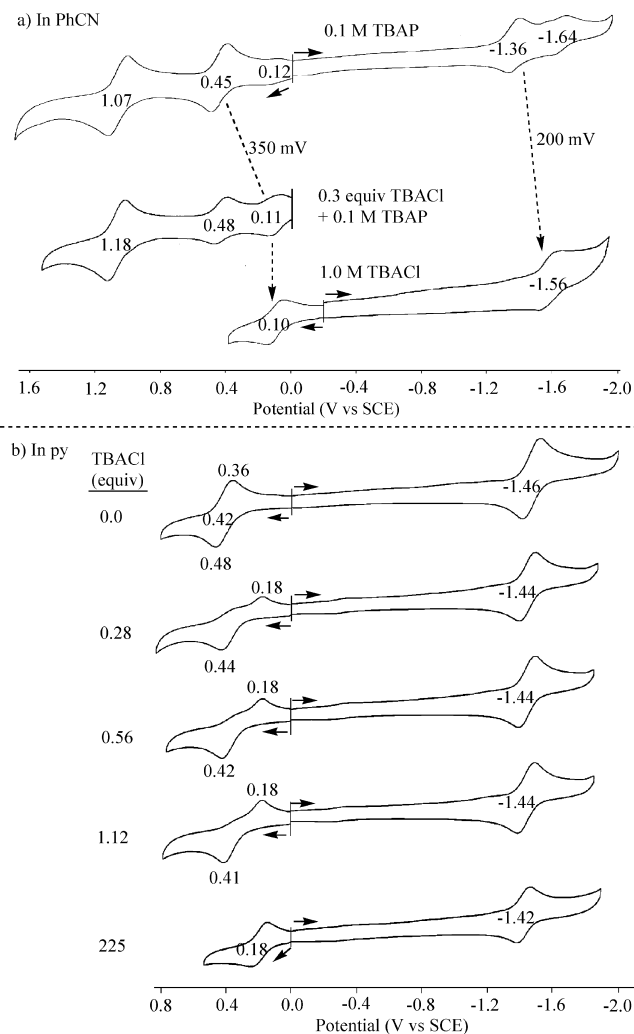

Figure 9. Cyclic voltammograms of (Mes₂PhCor)Mn **1** (1.7×10^{-3} M) in (a) PhCN containing (i) 0.1 M TBAP, (ii) 0.1 M TBAP and 0.3 equiv TBACl, and (iii) 1.0 M TBACl and (b) the same concentration of the corrole in pyridine with 0.1 M TBAP and added TBACl.

mV negative shift of potential. At the same time the first reduction in PhCN with 0.1 M TBACl occurs at $E_{1/2} = -1.56$ V as compared to −1.36 V when no Cl^- is present, a negative shift of 200 mV in half-wave potential.

After formation of the five-coordinate compound, the $E_{1/2}$ for oxidation is independent of additional chloride added to solution (see Figure 9a) and this would only occur if the number of axially bound anions on the initial Mn^{III} corrole and singly oxidized Mn^{IV} corrole were identical; otherwise one would expect a 60 mV shift in $E_{1/2}$ per each 10-fold
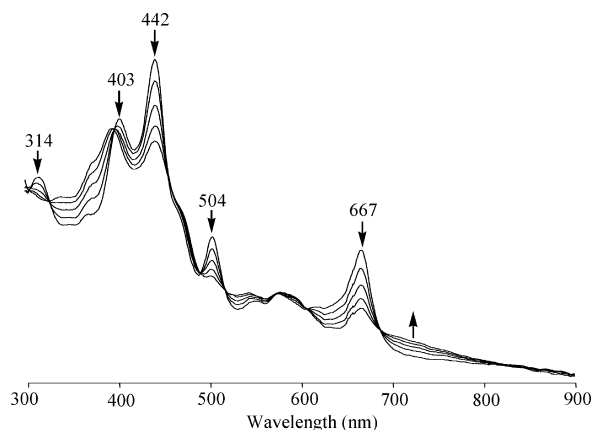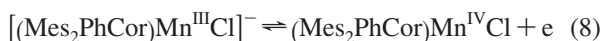

Figure 8. UV–visible spectral changes during controlled potential reduction of (Mes₂PhCor)Mn (**1**) in pyridine, 0.1 M TBAP at an applied potential of −1.80 V.

(58) Arasasingham, R. D.; Bruice, T. C. *Inorg. Chem.* **1990**, *29*, 1422–1427.
(59) Ramirez-Gutierrez, O.; Claret, J.; Ribo, J. M. *J. Porphyrins Phthalocyanines* **2005**, *9*, 436–443.
(60) Autret, M.; Ou, Z.; Antonioni, A.; Boschi, T.; Tagliatesta, P.; Kadish, K. M. *J. Chem. Soc., Dalton Trans.* **1996**, 2793–2797.
(61) Guilard, R.; Barbe, J.-M.; Boukhris, A.; Lecomte, C.; Anderson, J. E.; Xu, Q. Y.; Kadish, K. M. *J. Chem. Soc., Dalton Trans.* **1988**, 1109–1113.
(62) Kadish, K. M.; Xu, Q. Y.; Barbe, J.-M.; Anderson, J. E.; Wang, E.; Guilard, R. *Inorg. Chem.* **1988**, *27*, 691–696.
(63) Kadish, K. M.; Xu, Q. Y.; Barbe, J.-M.; Guilard, R. *Inorg. Chem.* **1988**, *27*, 1191–1198.

change in log[Cl⁻].[64] Thus, the invariance of $E_{1/2}$ with added Cl⁻ after the reversible oxidation potential has shifted from 0.45 to 0.10 V indicates that the prevailing electrode reaction on the time scale of the electrochemical measurement can be described by eq 8 in solutions of PhCN containing >0.3 equiv Cl⁻. Similar arguments were used for identifying[46] the redox-active site of the (TPFC)MnX/(TPFC)Mn couple as Mn^{IV}/Mn^{III} and that of the (TPP)FeX/(TPP)Fe[64] as Fe^{III}/Fe^{II}.

$$[(\text{Mes}_2\text{PhCor})\text{Mn}^{III}\text{Cl}]^- \rightleftharpoons (\text{Mes}_2\text{PhCor})\text{Mn}^{IV}\text{Cl} + e \quad (8)$$

The binding constant for addition of one Cl⁻ ligand to (Mes₂PhCor)Mn^{III} was calculated as $10^{4.8}$ from spectroscopic data of the type shown in Figure 6 for CN⁻ and OAc⁻ (see Supporting Information, Figure S3 for Cl⁻ titration results) and thus a combination of eq 8 with eq 2 enables calculation of the chloride binding constant to the Mn(IV) form of the corrole, that is, [(Mes₂PhCor)Mn^{IV}]⁺. The relevant electrochemical equation is $\Delta E_{1/2} = 0.059 \log(K_{Mn(IV)}/K_{Mn(III)})$[64] which leads to a $K_{Mn(IV)}/K_{Mn(III)}$ ratio of $10^{5.9}$ and a $\log K_{Mn(IV)}$ of $10^{10.7}$ for the chloride binding reaction given in eq 9.

$$[(\text{Mes}_2\text{PhCor})\text{Mn}^{IV}]^+ + \text{Cl}^- \rightleftharpoons (\text{Mes}_2\text{PhCor})\text{Mn}^{IV}\text{Cl} \quad (9)$$
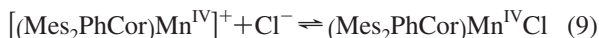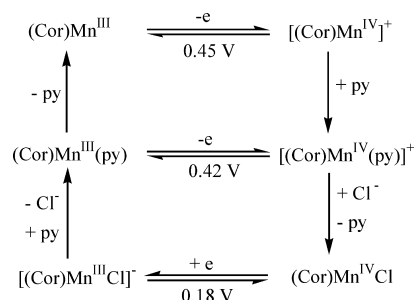
The large chloride binding constant to the Mn^{IV} corrole in PhCN suggests that Cl⁻ might also bind to the singly oxidized species in pyridine and indeed this is the case as demonstrated by the cyclic voltammograms in Figure 9. The first oxidation is reversible in PhCN and pyridine but not in pyridine containing low concentrations of added TBACl where a classic box mechanism is observed. Here the Mn^{III}/Mn^{IV} process is described by two related electrochemical EC mechanisms, each of which involves an electron transfer followed by a fast chemical reaction. The initial oxidation involves a one electron conversion of (Cor)Mn(py) to [(Cor)Mn(py)]⁺ followed by the rapid formation of (Cor)MnCl at the electrode surface. The halide bound species is harder to reduce than the uncoordinated species and after conversion of (Cor)MnCl to [(Cor)MnCl]⁻, the axial chloride ion dissociates giving again (Cor)Mn at the electrode surface and in solution. These reactions occur at the noncoupled peak potentials of 0.41 to 0.44 V for oxidation and 0.18 V for reduction as seen in the lower portion of Figure 9.
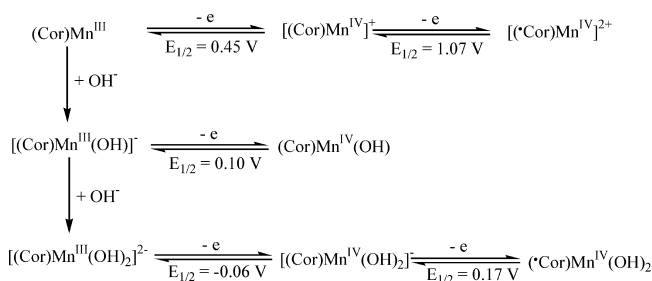
This mechanism for oxidation of (Mes₂PhCor)Mn **1** under the different solution conditions is summarized in Scheme 2 where the reversible electrode reactions are observed in neat PhCN (0.45 V), neat pyridine (0.42 V), and pyridine containing >225 equiv of added TBACl.

Acetate and Hydroxide Effect on Electrooxidation in PhCN. The effect of adding acetate or hydroxide ions to **1** in PhCN is similar to what is seen upon addition of Cl⁻ or CN⁻. In each case the anionic [(Cor)MnX]⁻ species in solution is easier to oxidize than uncharged (Cor)Mn, these reactions occurring at $E_{1/2} = 0.30$ V in the case of OAc⁻ and 0.04 V in the case of CN⁻, the relevant electron transfer

(64) Kadish, K. M. In *Iron Porphyrins II*; Lever, A. B. P., Gray, H. B., Eds.; Addison-Wesley Publishing Company, Inc.: Canada, 1983, pp 161−249.

Scheme 2

Scheme 3

reactions being given by eq 8. A six-coordinate Mn^{IV} species with bound OAc⁻ or OH⁻ is the final electrooxidation product, and both corroles can be reduced back to Mn(III) at similar potentials of −0.06 and −0.08 V. [(Mes₂PhCor)Mn(OH)]$^{2-}$ is stable and can be reversibly oxidized and reduced but not the electrogenerated [(Cor)Mn(OAc)]$^{2-}$ which rapidly loses one axial ligand, giving the irreversible redox process shown by the cyclic voltammogram in Figure 10b.

The relevant electron transfer mechanism in the case of OH⁻ is given in Scheme 3 where $E_{1/2} = 0.10$ V for the reversible oxidation of [(Cor)Mn(OH)]⁻ to (Cor)Mn^{IV}(OH) and then, as [(Mes₂PhCor)Mn^{III}(OH)₂]$^{2-}$ is formed at higher concentrations of OH⁻, the prevailing redox process switches
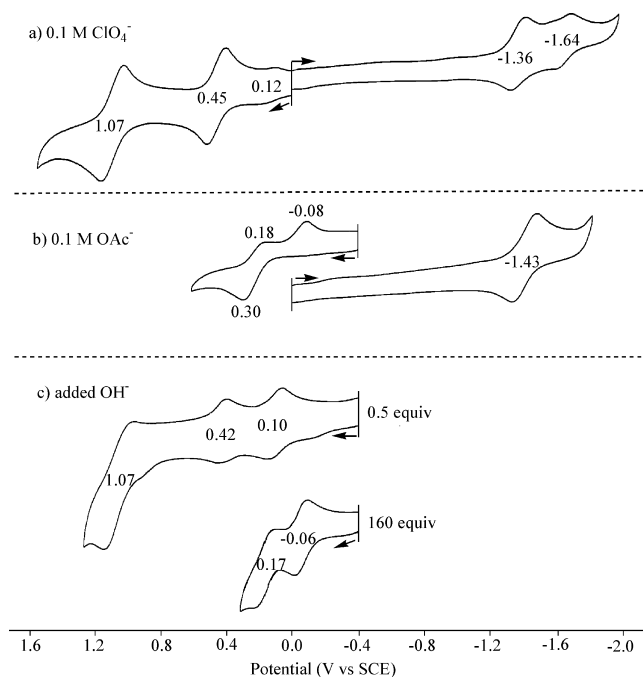
Figure 10. Cyclic voltammograms of (Mes₂PhCor)Mn **1** in PhCN with (a) 0.1 M ClO₄⁻, (b) 0.1 M OAc⁻, and (c) added OH⁻.

Scheme 4

to an $E_{1/2}$ of -0.06 V, consistent with an easier oxidation of the dianionic species. At the same time, the electrogenerated $[(Cor)Mn^{IV}(OH)_2]^{2-}$ is also easier to oxidize, and the $E_{1/2}$ for this process shifts from 1.07 V in solutions with 0.1 M TBAP and 0.5 equiv OH$^-$ to 0.17 V in PhCN containing 0.1 M TBAP and 160 equiv TBAOH. This is a remarkable shift in potential, a high stability of the doubly oxidized corrole, and is similar to what was previously reported after chloride titrations of a similar compound in CH_2Cl_2.[33]

As mentioned above, the oxidation of $[(Cor)Mn^{III}(OAc)]^-$ to $(Cor)Mn^{IV}(OAc)$ is followed by addition of a second axial ligand in solutions with high acetate concentrations, and the bis-acetate adduct formed as a result of this electrochemical EC mechanism can then be reduced to $[(Cor)Mn^{III}(OAc)_2]^{2-}$, followed by loss of one OAc$^-$ ligand giving again the original five-coordinate species by a second EC mechanism. This classic electrochemical box mechanism is shown in Scheme 4 where the reversible electron transfer reactions occur at 0.30 and -0.08 V prior to the addition or loss of an axial ligand.

Finally, the half-wave potentials for each examined mono- and bis-adduct in PhCN are summarized in Table 3. The monoadducts can all be reversibly oxidized at $E_{1/2}$ valves of 0.04 to 0.30 V and reversibly reduced at potentials of -1.43 to -1.66 V, the latter potential being for the mono-OH$^-$ complex. Reductions could not be observed in solutions with high concentrations of the anionic ligand, perhaps because this reaction would occur at very negative potentials if the axial ligand were lost after reduction, the expected shift in

Table 3. $E_{1/2}$ Values of $(Mes_2PhCor)Mn$ **1** Complexes in PhCN Containing added Anions

formula	X$^-$ (conc.)	first ox Mn$^{III/IV}$	first red Mn$^{III/II}$
$(Mes_2PhCor)Mn$	none	0.45	-1.36
$[(Mes_2PhCor)MnX]^-$	CN$^-$ (1.6 equiv)	0.04	-1.46
	Cl$^-$ (1.0 M)	0.10	-1.56
	OH$^-$ (1.9 equiv)	0.10	-1.66
	OAc$^-$ (0.1 M)	0.30[a]	-1.43
$[(Mes_2PhCor)MnX_2]^{2-}$	OAc$^-$ (0.1 M)	-0.08[a]	
	OH$^-$ (400 equiv)	-0.06	

[a] Peak potential at a scan rate of 0.1 V/s.

$E_{1/2}$ from the uncomplexed species amounting to -60 to -120 mV per each 10-fold change in axial ligand concentration.

In summary, a series of *meso*-substituted manganese(III) corroles were investigated as to their electrochemical, spectroelectrochemical, and anion binding properties in nonaqueous solvents. The Mn(II) and Mn(IV) forms of the corroles could be electrogenerated by controlled potential oxidation or reduction. Five- or six-coordinate complexes were *in situ* generated depending upon the specific anions added to solution in the form of a TBA$^+$ salt. Complexation with one or two anionic axial ligands led to an easier oxidation and a harder reduction in each case as compared to the uncomplexed four-coordinated species.

Supporting Information Available: Table of UV−visible spectra of neutral compound, $(Mes_2PhCor)Mn$, in different solvents, spectra of SCN$^-$ and Cl$^-$ bound species in PhCN and spectroelectrochemistry data in DMSO. This material is available free of charge via the Internet at http://pubs.acs.org.

IC8007415